Supporting Information

1- Molecular Structure and Magnetic Properties of 1-Ethyl-2-(1-oxyl-3-oxo-4,4,5,5-tetramethylimidazolin-2-yl)-3-methylimidazolium Arylcarboxylates and Other Salts

Hiroyuki Hayashi, Satoru Karasawa, and Noboru Koga*

Graduate School of Pharmaceutical Sciences, Kyushu University, 3-1-1 Maidashi, Higashi-ku, Fukuoka, 812-8582 Japan. koga@fc.phar.kyushu-u.ac.jp

Table of Contents

S7. ESR spectra of $[EMINN]^{+}_{2}[BA_2]^{2-}$ and $[EMINN]^{+}_{3}[BA_3]^{3-}$ in 5 % EtOH/toluene at room temperature. (Figure S6)

S1. **General Methods.** Infrared spectra were recorded on a FT-IR spectrometer. ^{1}H NMR spectra were measured on a 270 MHz spectrometer using $CDCl_3$ as solvent and referenced to TMS. FAB mass spectra (FAB MS) were recorded on a spectrometer and ESI mass spectra were measured on a spectrometer in the positively charged mode. Melting points were obtained with a heating block and are uncorrected. Elemental analyses were performed in the Analytical Center of Faculty of Science in Kyushu University.

S2. ORTEP drawing (Figure S1)

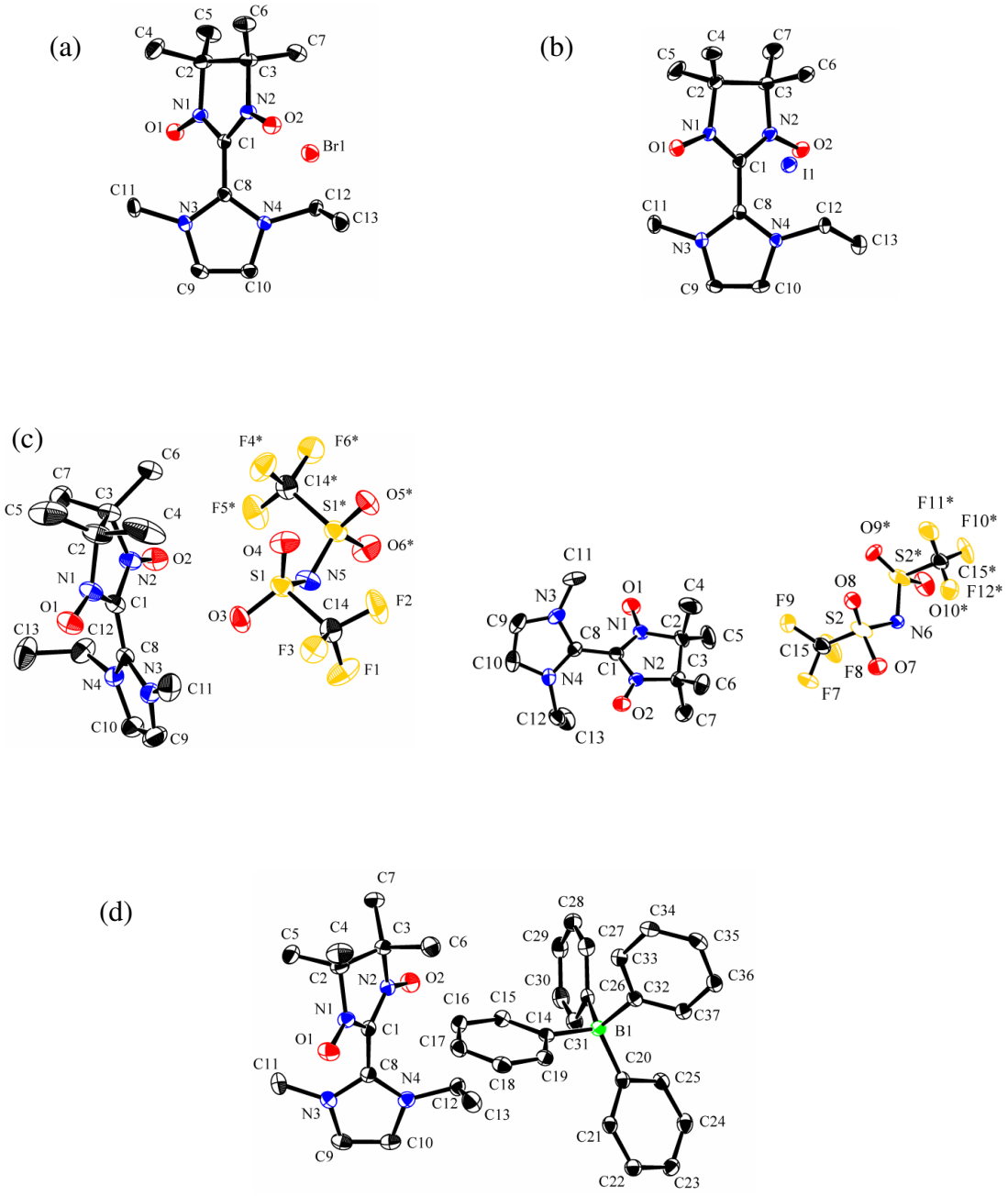

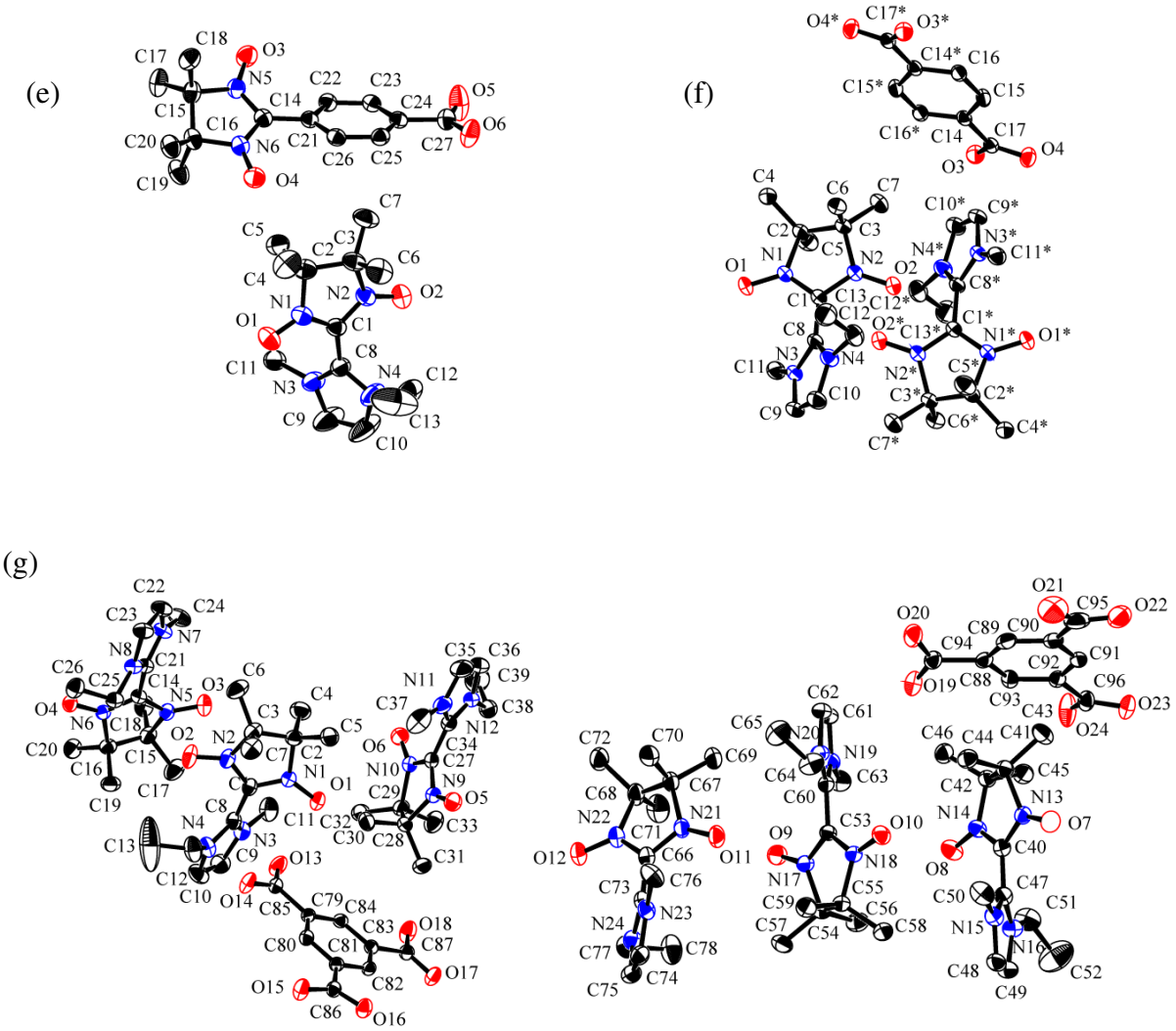

Figure S1. ORTEP drawings of (a) $[EMINN]^+[Br]^-$, (b) $[EMINN]^+[I]^-$, (c) $[EMINN]^+[TFSI]^-$, (d) $[EMINN]^+[BPh_4]^-$, (e) $[EMINN]^+[BANN]^-$, (f) $[EMINN]^+_2[BA_2]^{2-}$, and (g) $[EMINN]^+_3[BA_3]^{3-}$

Table S1. Crystallographic data and experimental details for $[EMINN]^+[X]^-$, X = Br, I, TFSI, and BPh_4.

	$[EMINN]^+[Br]^-$	$[EMINN]^+[I]^-$	$[EMINN]^+[TFSI]^-$	$[EMINN]^+[BPh_4]^-$
empirical formula	$C_{13}H_{22}O_2N_4Br$	$C_{13}H_{22}O_2N_4I$	$C_{15}H_{22}F_6O_6N_5S_2$	$C_{37}H_{42}O_2N_4B$
formula weight	346.25	393.25	546.48	585.57
crystal class	monoclinic	monoclinic	triclinic	monoclinic
space group	$P2_1/c$ (No.14)	$P2_1/n$ (No.14)	P-1 (No.2)	$P2_1/c$ (No.14)
a /Å	8.1985(3)	8.329(7)	10.041(3)	11.0929(4)
b /Å	9.3294(4)	9.432(9)	10.534(4)	13.9282(5)
c /Å	21.0272(6)	21.42(2)	12.180(4)	20.9843(6)
α/deg			67.590(9)	
β/deg	102.2128(9)	101.58(4)	80.391(7)	103.0763(10)
γ/deg			85.956(9)	
V /Å^3	1571.91(9)	1648.8(26)	1174.3(7)	3158.10(18)

μ /cm^{-1}	26.303	19.505	3.152	0.762
Z	4	4	2	4
crystal size / mm	0.40 x 0.30 x 0.30	0.50 x 0.40 x 0.30	0.80 x 0.70 x 0.60	0.40 x 0.40 x 0.20
D_{calc}/gcm^{-3}	1.463	1.584	1.545	1.231
F(000)	716.00	788.00	562.00	1252.00
radiation	Mo-K$_\alpha$	Mo-K$_\alpha$	Mo-K$_\alpha$	Mo-K$_\alpha$
T/K	138	123	123	130
no. reflections measured	6138	7125	11369	14033
no. unique reflections	3421	3761	5263	7154
no. reflections observed	3421(all)	3761(all)	5263(all)	7154(all)
no. parameters	270	182	495	566
R_1	0.0358	0.0299	0.0483	0.0539
wR_2	0.0946	0.0789	0.1431	0.1345
GOF	1.058	0.950	1.120	1.043

[a] $R_1 = \Sigma \, ||F_0|-|F_c|| / \Sigma \, |F_0|$; $wR_2 = \{ \Sigma \, w(F_0^2-F_c^2)^2 / \Sigma \, w(F_0^2)^2 \}^{1/2}$

Table S2. Crystallographic data and experimental details for [EMINN]$^+$[BANN]$^-$, [EMINN]$^+_2$[BA$_2$]$^{2-}$, and [EMINN]$^+_3$[BA$_3$]$^{3-}$.

	[EMINN]$^+$[BANN]$^-$	[EMINN]$^+_2$[BA$_2$]$^{2-}$	[EMINN]$^+_3$[BA$_3$]$^{3-}$
empirical formula	$C_{27}H_{38}O_6N_6 \cdot 1.5\ H_2O$	$C_{34}H_{48}O_8N_8 \cdot 4\ H_2O$	$C_{48}H_{69}O_{12}N_{12} \cdot 10\ H_2O$
formula weight	568.65	768.86	1166.14
crystal class	monoclinic	triclinic	triclinic
space group	P2$_1$/c (No.14)	P-1 (No.2)	P-1 (No.2)
a /Å	6.1258(3)	8.3259(5)	16.875(5)
b /Å	35.4226(17)	10.4511(7)	20.251(5)
c /Å	13.6162(7)	12.6849(9)	20.322(5)
α/deg		69.5550(19)	59.287(5)
β/deg	95.8160(19)	75.3050(18)	85.537(5)
γ/deg		77.6580(16)	79.624(5)
V /Å^3	2939.4(3)	990.83(12)	5872(3)
μ /cm^{-1}	0.947	0.981	1.051
Z	4	1	4
crystal size / mm	0.8 x 0.40 x 0.10	0.40 x 0.30 x 0.30	0.6 x 0.50 x 0.40
D_{calc}/gcm^{-3}	1.285	1.288	1.319
F(000)	1216.00	412.00	2468.00
radiation	Mo-K$_\alpha$	Mo-K$_\alpha$	Mo-K$_\alpha$
T/K	123	133	133
no. reflections measured	26969	7071	43631
no. unique reflections	6370	4306	24146
no. reflections observed	6370(all)	4306(all)	24146(all)
no. parameters	371	261	1478
R_1	0.0630	0.0650	0.0728
wR_2	0.1821	0.2258	0.1042
GOF	1.084	1.061	1.079

[a] $R_1 = \Sigma \, ||F_0|-|F_c|| / \Sigma \, |F_0|$; $wR_2 = \{ \Sigma \, w(F_0^2-F_c^2)^2 / \Sigma \, w(F_0^2)^2 \}^{1/2}$

S3. Crystal structure (Figure S2)

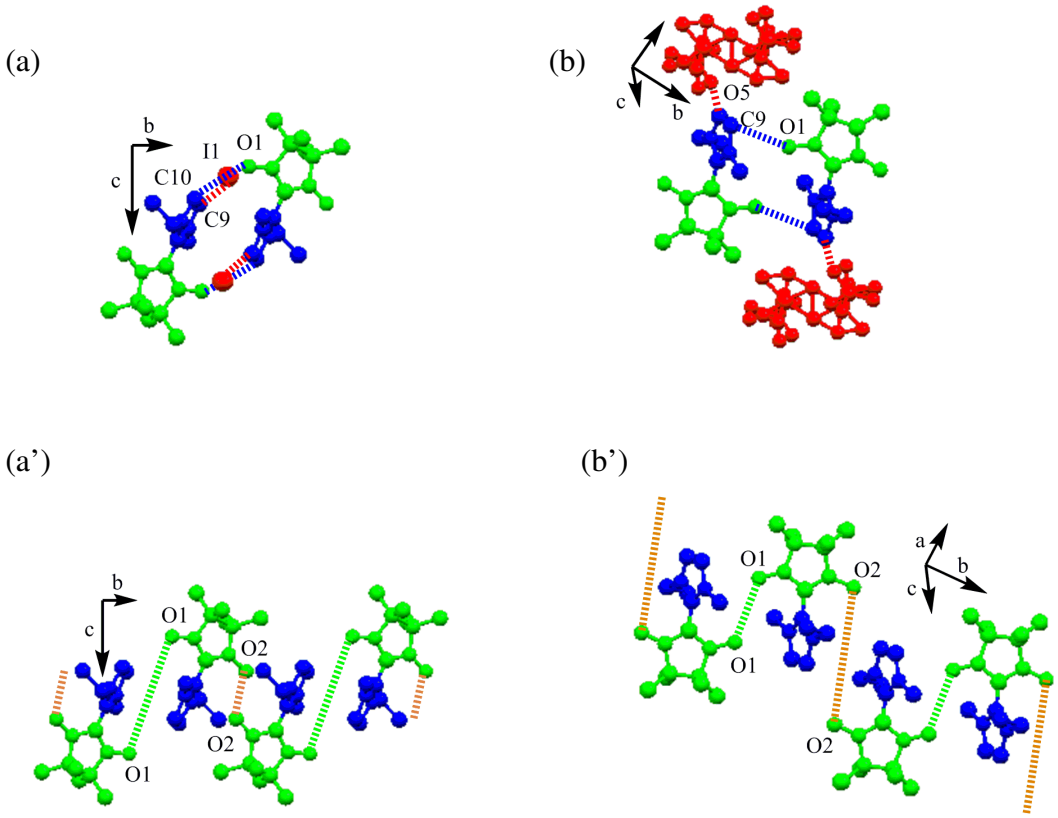

Figure S2. Dimer structure (upper) and packing diagram (lower) with a ball-stick model (color code: NN moiety, green; Im-cation, blue; anion, red) for ((a) and (a'), respectively) $[EMINN]^+[I]^-$ and ((b) and (b'), respectively) $[EMINN]^+[TFSI]^-$. In (a) and (b), the short O(NN)-C(Im) and anion-C(Im) contacts within the dimers are indicated by the blue and red dashed lines, respectively. In (a') and (b'), the anion units are omitted for the sake of clarity and the short NO-NO contacts within and between dimers are indicated by the green and orange dashed lines, respectively.

S4. the $\chi_{mol}T$ vs. T plots of $[EMINN]^+[I]^-$ and $[EMINN]^+[TFSI]^-$ (Figure S3)

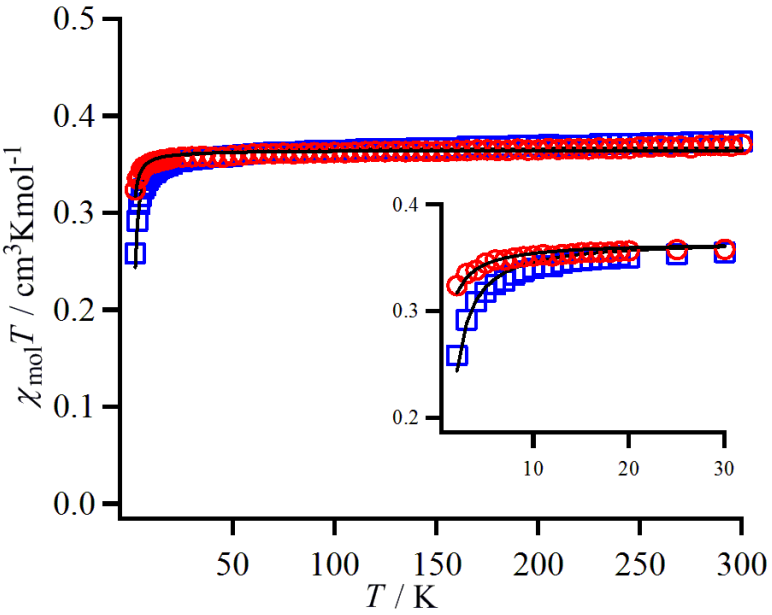

Figure S3. Plots of $\chi_{mol}T$ vs. T of $[EMINN]^+[I]^-$ ○) and $[EMINN]^+[TFSI]^-$ □). The slid lines are fitting theoretical curves with the optimized parameters.

S5. ESI mass spectra (Figure S4)

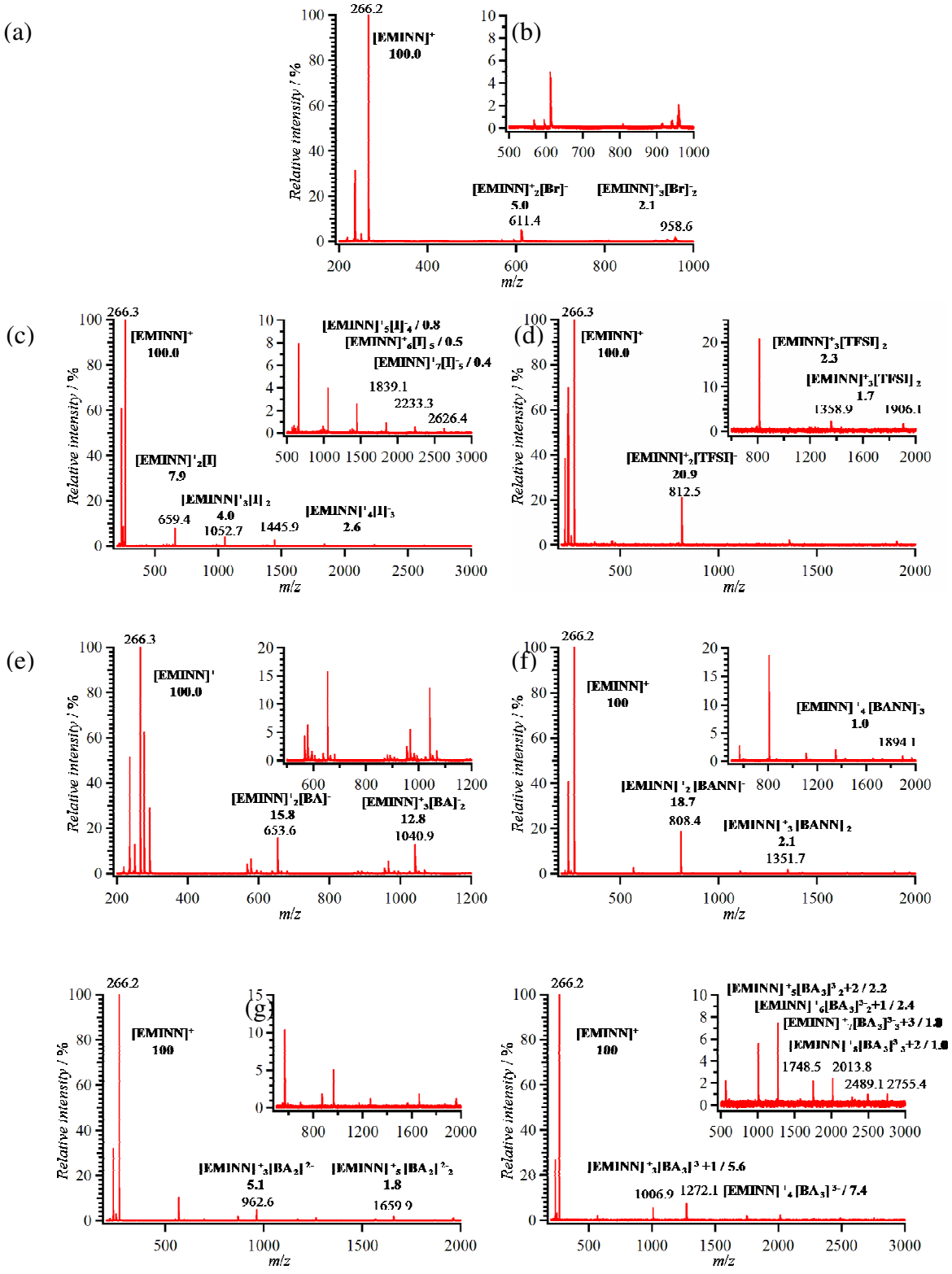

Figure S4. ESI mass spectra of (a) $[EMINN]^+[Br]^-$, (b) $[EMINN]^+[I]^-$, (c) $[EMINN]^+[TFSI]^-$, (d) $[EMINN]^+[BA]^-$, (e) $[EMINN]^+[BANN]^-$, (f) $[EMINN]^+_2[BA_2]^{2-}$, and (g) $[EMINN]^+_3[BA_3]^{3-}$

S6. the spin-lattice and the spin-spin relaxation rate ($1/T_1$ and $1/T_2$) in solution (Figure S5)

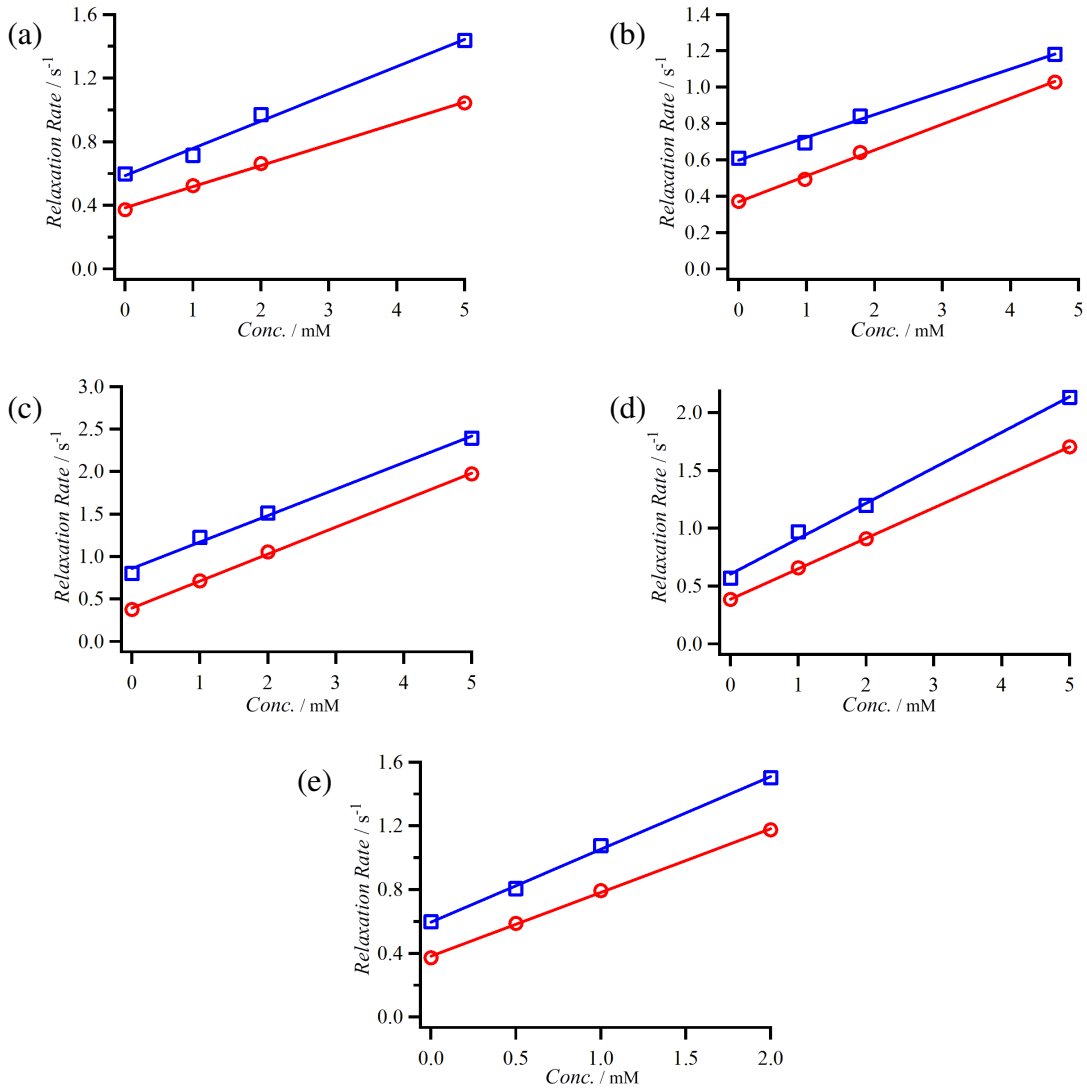

Figure S5. The plots of $1/T_1$(○) and $1/T_2$(□) vs. Conc. of (a) $[EMINN]^+[Br]^-$, (b) $[EMINN]^+[BA]^-$, (c) $[EMINN]^+[BANN]^-$, (d) $[EMINN]^+_2\,[BA_2]^{2-}$, and (e) $[EMINN]^+_3\,[BA_3]^{3-}$ in aqueous solution. The solid lines are fitting theoretical curves with the optimized parameters. See in the text.

S7. ESR spectra of $[EMINN]^{+}_{2}[BA_2]^{2-}$ and $[EMINN]^{+}_{3}[BA_3]^{3-}$ (Figure S6)

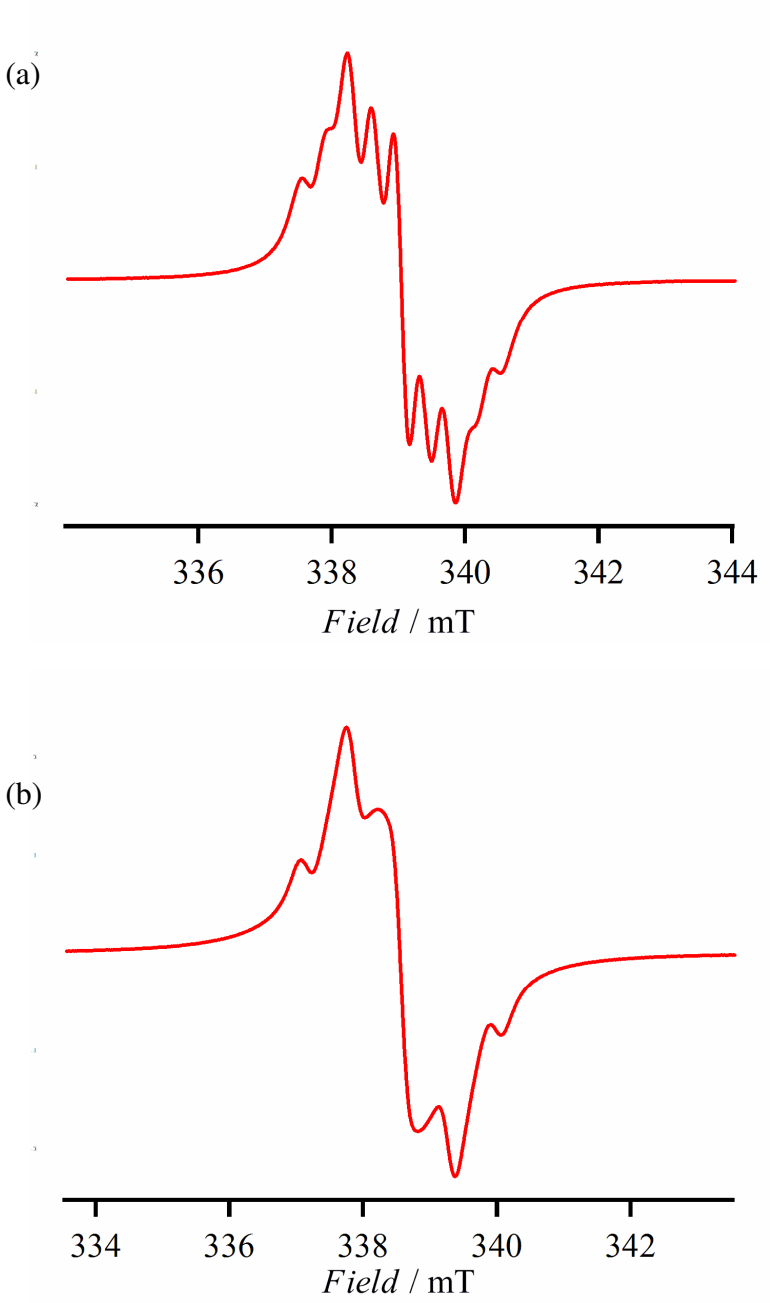

Figure S6. ESR spectra (1mM) of (a) $[EMINN]^{+}_{2}[BA_2]^{2-}$ and (b) $[EMINN]^{+}_{3}[BA_3]^{3-}$ in 5 % EtOH/toluene at room temperature.